ISSN 1070-3284, Russian Journal of Coordination Chemistry, 2018, Vol. 44, No. 12, pp. 818–823. © Pleiades Publishing, Ltd., 2018.

A New Heterometallic Pb(II)–Ca(II) Coordination Polymer with 2D Pb–O–Ca Inorganic Connectivity[1]

Z. An[a], J. Gao[b], and J. Wang[c], *
[a]*School of Chemical Engineering, Guangdong University of Petrochemical Technology, Maoming, Guangdong Province, 525000 P.R. China*
[b]*Department of Pharmacy, Mudanjiang Medical University, Mudanjiang, Heilongjiang Province, 157011 P.R. China*
[c]*School of Environmental and Biological Engineering, Guangdong University of Petrochemical Technology, Maoming, Guangdong Province, 525000 P.R. China*
**e-mail: zheanngsh@163.com*

Received March 4, 2018

Abstract—A new heterometallic-organic framework, namely $[PbCa(Mbdc)_2(DMF)]_n$ (**I**) (H_2Mbdc = isophthalic acid, DMF = *N*,*N*'-dimethylformamide), was synthesized by the solvothermal reactions of $Pb(NO_3)_2$, $Ca(NO_3)_2 \cdot 4H_2O$ and H_2Mbdc. Single crystal X-ray diffraction analysis (CIF file CCDC no. 1567197) revealed that compound **I** features a 3D pillar-layered framework with 2D inorganic Pb–O–Ca connectivity. Thermal analysis indicated that the framework of compound **I** can be stable up to 320°C, and luminescent property investigation indicated that compound **I** exhibits intense luminescence at room temperature.

Keywords: solvothermal reactions, heterometallic compound, inorganic connectivity, luminescence
DOI: 10.1134/S1070328418120011

INTRODUCTION

During the past few decades, metal-organic frameworks (MOFs) have received considerable attention not only owing to their aesthetically beautiful structural features and interesting topologies but also owing to their potential applications as functional materials in the fields of luminescence sensing, gas storage and separation, heterogeneous catalysis, magnetism and so on [1–6]. It is well known that the MOFs are assembled by the central metal ions and multifunctional organic ligands under driving power of coordination. Therefore, the selection of metal ions and organic ligands is very important to insure desirable properties and expected structures of MOFs [7, 8]. Up to now, the synthesized MOFs are mainly based on *s*-, *d*-, and *f*-block metal coordination centers [9–12]. Comparatively speaking, *p*-block metal ions, despite they have important applications in electroluminescent devices and photovoltaic conversion, gained less attention for the construction of MOFs [13–15]. Lead(II), as a *p*-block metal ion, has relative large ionic radius and strong affinity to oxygen-donors, making them adopt variable coordination geometries (hemidirected geometry and holodirected geometry) in the assemble process [16–18]. Thus, organic multicarboxylate ligands are widely used for the construction of lead(II)-based MOFs, and lots of lead(II)-aromatic carboxylate crystalline materials with varied 1D to 3D inorganic Pb–O–Pb connectivities have been successfully obtained [19–21]. In addition, alkaline earth metal ions have strong affinity to oxygen donors, and also can be bridged by the multicarboxylate ligand into functional MOFs [22–24]. So the incorporation of alkaline earth metal ions into the system of lead(II) ions and organic multicarboxylic acid may afford new heterometallic hybrid materials with varied inorganic Pb–O–M (M = Ca, Sr or Ba) connectivities [25]. In viewing that, in this work, we selected isophthalic acid as the organic building blocks to assemble with lead(II) ions and calcium(II) ions under solvothermal conditions, successfully obtaining a new heterometallic compound, namely $[PbCa(Mbdc)_2(DMF)]_n$ (**I**) (H_2Mbdc = isophthalic acid, DMF = *N*,*N*'-dimethylformamide). Single crystal X-ray diffraction analysis revealed that this compound features a 3D pillar-layered framework with 2D inorganic Pb–O–Ca connectivity.

EXPERIMENTAL

Materials and methods. All the starting materials and reagents used in this work were obtained commercially and used without further purification. Element analyses (C, H and N) were determined with an elemental Vairo EL III analyzer. Infrared spectra using the KBr pellets were measured on a Nicolet Magna 750 FT-IR spectrometer in the range of 400–4000 cm^{-1}. Powder X-ray diffraction (PXRD) data

---

[1] The article is published in the original.

Table 1. Crystallographic data and structure refinements for complex **I**

Parameter	Value
Empirical formula	$C_{19}H_{15}NO_9CaPb$
Temperature, K	293(2)
Crystal color	Colorless
Formula weight	648.6
Crystal system	Monoclinic
Space group	$P2_1/c$
a, Å	10.1806(8)
b, Å	12.6199(10)
c, Å	16.5087(15)
β, deg	101.090(10)
V, Å^3	2081.4(3)
Z	4
ρ_{calcd}, g/cm^3	2.070
μ, mm^{-1}	8.404
F(000)	2959
θ Range for data collection, deg	2.51 to 25.00
Reflections collected	7603
Unique reflections	3642
R_{int}	0.0406
Goodness-of-fit on F^2	1.140
R_1, wR_2 ($I > 2\sigma(I)$)	0.0851, 0.2034
R_1, wR_2 (all data)	0.0943, 0.2079

were collected using PANalytical X'Pert Pro powder diffractometer with CuK_α radiation and $5° \le 2\theta \le 50°$. Thermogravimetric (TG) analysis was carried out on a NetzschSTA499C integration thermal analyzer under a nitrogen atmosphere from 30 to 800°C at a heating rate of 10°C/min. Fluorescent spectra for the solid-state samples were performed on an Edinburgh Analytical Instrument FLS920.

Synthesis of complex I. A mixture of $Pb(NO_3)_2$ (0.033 g, 0.1 mmol), $Ca(NO_3)_2 \cdot 4H_2O$ (0.018 g, 0.1 mmol), H_2Mbdc (0.034 g, 0.20 mmol), H_2O (2 mL), DMF (3 mL) and 2 drops concentrated nitric acid was placed in a 20 mL glass vial, and then glass vial was transfer into an oven and kept at 110°C for three days. After being slowly cooled to the room temperature, colorless block crystals of **I** were isolated. The yield was 47% based on Pb(II).

For $C_{19}H_{15}NO_9CaPb$ ($M = 648.6$)

Anal. calcd., %	C, 35.42	H, 3.84	N, 4.13
Found, %	C, 35.44	H, 3.79	N, 4.16

IR (KBr; ν, cm^{-1}): 3427 w, 1652 w, 1563 s, 1477 w, 1412 m, 1384 s, 1267 w, 1158 w, 1031 w, 958 w, 832 w, 784 s.

X-ray crystallography. A single crystal structure analysis of **I** was performed on Oxford Xcalibur E diffractometer (MoK_α radiation, λ = 0.71073 Å, graphite monochromator) at 293(2) K. Empirical absorption corrections were applied to the data using the SADABS program [26]. The structure was solved by the direct method and refined by the full-matrix least-squares on F^2 using the SHELXL-97 program [27]. All of the non-hydrogen atoms were refined anisotropically, and the hydrogen atoms attached to carbon atoms were located at their ideal positions. Experimental details for the structure determination are presented in Table 1. Selected bond lengths and angles for compound **I** are listed in Table 2.

Supplementary material for complexes has been deposited with the Cambridge Crystallographic Data Centre (CCDC no. 1567197; deposit@ccdc.cam.ac.uk or http://www.ccdc.camac.uk).

Table 2. Selected bond lengths (Å) and angles (deg) for compound **I***

Bond	*d*, Å	Bond	*d*, Å
Pb(1)–O(6)	2.577(14)	Pb(1)–O(3)$^{\#2}$	2.588(17)
Pb(1)–O(4)$^{\#2}$	2.660(14)	Pb(1)–O(5)$^{\#1}$	2.698(14)
Pb(1)–O(2)	2.711(14)	Pb(1)–O(1)	2.754(19)
Pb(1)–O(7)$^{\#3}$	2.8569(14)	Pb(1)–O(8)$^{\#3}$	2.8093(14)
Ca(1)–O(9)	2.272(19)	Ca(1)–O(2)	2.287(13)
Ca(1)–O(8)	2.295(14)	Ca(1)–O(5)$^{\#4}$	2.306(14)
Ca(1)–O(4)$^{\#2}$	2.307(13)	Ca(1)–O(7)$^{\#3}$	2.322(15)
Angle	ω, deg	Angle	ω, deg
O(6)Pb(1)O(3)$^{\#2}$	87.9(6)	O(6)Pb(1)O(4)$^{\#2}$	79.5(4)
O(3)$^{\#2}$Pb(1)O(4)$^{\#2}$	50.2(4)	O(6)Pb(1)O(5)$^{\#1}$	119.3(4)
O(3)$^{\#2}$Pb(1)O(5)$^{\#1}$	82.7(4)	O(4)$^{\#2}$Pb(1)O(5)$^{\#1}$	130.0(4)
O(6)Pb(1)O(2)	87.1(5)	O(3)$^{\#2}$Pb(1)O(2)	119.2(4)
O(4)$^{\#2}$Pb(1)O(2)	69.4(4)	O(5)$^{\#1}$Pb(1)O(2)	147.6(4)
O(6)Pb(1)O(1)	87.5(5)	O(3)$^{\#2}$Pb(1)O(1)	166.9(5)
O(4)$^{\#2}$Pb(1)O(1)	116.8(4)	O(5)$^{\#1}$Pb(1)O(1)	110.2(5)
O(2)Pb(1)O(1)	48.3(4)	O(7)$^{\#3}$Pb(1)O(8)$^{\#3}$	44.968(3)
O(9)Ca(1)O(2)	169.5(6)	O(9)Ca(1)O(8)	100.1(6)
O(2)Ca(1)O(8)	90.0(6)	O(9)Ca(1)O(5)$^{\#4}$	85.2(6)
O(2)Ca(1)O(5)$^{\#4}$	94.3(5)	O(8)Ca(1)O(5)$^{\#4}$	79.0(5)
O(9)Ca(1)O(4)$^{\#2}$	98.6(6)	O(2)Ca(1)O(4)$^{\#2}$	83.4(5)
O(8)Ca(1)O(4)$^{\#2}$	92.3(5)	O(5)$^{\#4}$Ca(1)O(4)$^{\#2}$	171.0(5)
O(9)Ca(1)O(7)$^{\#3}$	91.0(6)	O(2)Ca(1)O(7)$^{\#3}$	79.4(6)
O(8)Ca(1)O(7)$^{\#3}$	166.0(5)	O(5)$^{\#4}$Ca(1)O(7)$^{\#3}$	110.7(5)
O(4)$^{\#2}$Ca(1)O(7)$^{\#3}$	77.5(5)		

* Symmetry codes: $^{\#1}$ $-5 - x, -2 - y, 1 - z$; $^{\#2}$ $-1 + x, y, z$; $^{\#3}$ $-5 - x, 0.5 + y, 0.5 - z$; $^{\#4}$ $x, -2.5 - y, -0.5 + z$.

RESULTS AND DISCUSSION

Single crystal X-ray diffraction analysis indicated that compound **I** features a 3D framework with 2D inorganic Pb–O–Ca connectivity. The asymmetric unit of **I** contains one Pb^{2+} ion, one Ca^{2+} ion, two Mbdc^{2-} ligands and one coordinated DMF molecule. As shown in Fig. 1, the Pb(1) ion locates in a holodirected coordination sphere, which is completed by nine carboxylate oxygen atoms from five different Mbdc^{2-} ligands, and the Ca(1) ion locates in an octahedral coordination environment, which is defined by five carboxylate oxygen atoms and one coordinated DMF molecule. The Pb–O and Ca–O bond lengths are in the range of 2.577(1)–2.857(1) and 2.272(1)–2.322(1) Å, respectively, which are comparable with previously reported Pb(II) or Ca(II) compounds [28]. The Mbdc^{2-} ligand in **I** displays two different coordination modes (Fig. 2).

It is noteworthy that two adjacent Pb(1)O(9) polyhedrons are connected into a Pb(2)O(16) dimer via sharing one corner, and each Pb(2)O(16) dimer is surrounded by four Ca(1)O(8) octahedrons via sharing two plans and two cornerns. These connection modes resulted in a 2D Pb–O–Ca inorganic layer (Fig. 3a). Finally, these adjacent 2D Pb–O–Ca inorganic layers are bridged together by the Mbdc^{2-} ligands, giving rise to a 3D pillar-layer framework (Fig. 3b).

The PXRD analysis for compound **I** reveals that the experimental pattern corresponds well with the simulated pattern based on the single crystal diffraction data, indicating that the bulk samples of compound **I** are in single phase. The TG analysis was also performed to evaluate the thermal stability of compound **I** (Fig. 4). In the TG curve of compound **I**, the first weight loss of 11.12% occurred in the temperature range of 30–112°C, which is consistent with the loss of one coordinated DMF molecule per unit cell (calcd.

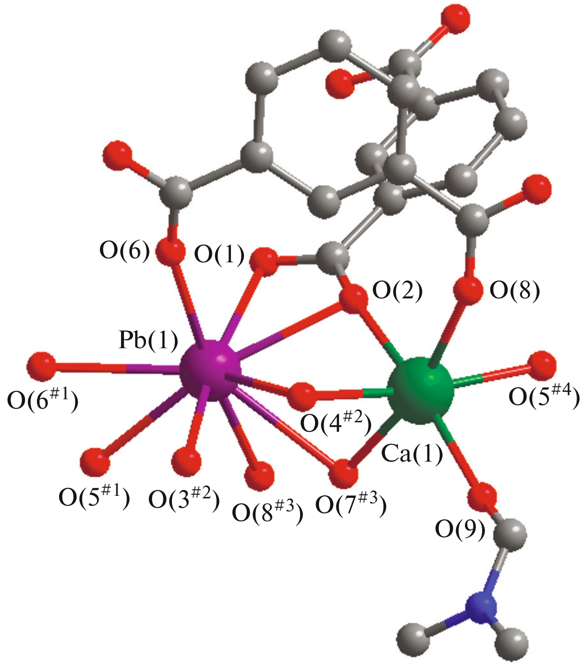

Fig. 1. The coordination environments around Pb^{2+} and Ca^{2+} ions in **I**, all hydrogen atoms were omitted for clarity (symmetry codes: $^{\#1}$ $-5-x, -2-y, 1-z$; $^{\#2}$ $-1+x, y, z$; $^{\#3}$ $-5-x, 0.5+y, 0.5-z$; $^{\#4}$ $x, -2.5-y, -0.5+z$).

11.26%). Then, the skeleton of compound **I** can be stable up to 325°C without any obvious weight loss. When the temperature was beyond 325°C, continuous weight loss was observed owing to the decomposition of the compound. The final residue of 43.12% might be the mixture of lead oxide and calcium oxide (calcd. 43.02%).

Considering the interesting photochemical and photophysical properties of Pb(II)-organic compounds, the solid-state emission spectra of compound **I** and free H_2Mbdc ligand have been investigated at room temperature. As shown in Fig. 5, compound **I** has an emission band with the maximum emission peak at 487 nm ($\lambda_{ex} = 325$ nm), and the free H_2Mbdc ligand shows an emission band centered at 368 nm ($\lambda_{ex} = 330$ nm). The emission band of 368 nm for H_2Mbdc ligand may be resulted by the intraligand $\pi \to \pi^*$ charge transition [29], and the emission band at 487 nm for compound **I** may be attributed to ligand-to-metal charge transfer (LMCT) between delocalized π bond of H_2Mbdc ligand and *p* orbitals of central Pb^{2+} ions [30]. In addition, the luminescent property of the desolvated samples was also investigated at the same conditions. As shown in Fig. 5, the desolvated samples showed more intense luminescence than that of com-

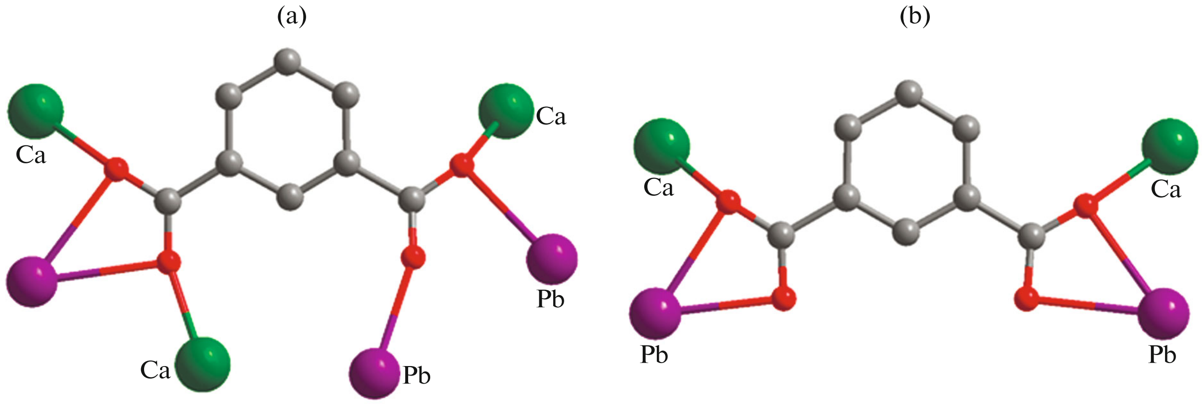

Fig. 2. Two different coordination modes of the $Mbdc^{2-}$ ligand in **I**: (μ_2-μ_2)-(μ_2-μ_2)-μ_6 (a) and (κ^2-μ_2)-(κ^2-μ_2)-μ_4 (b).

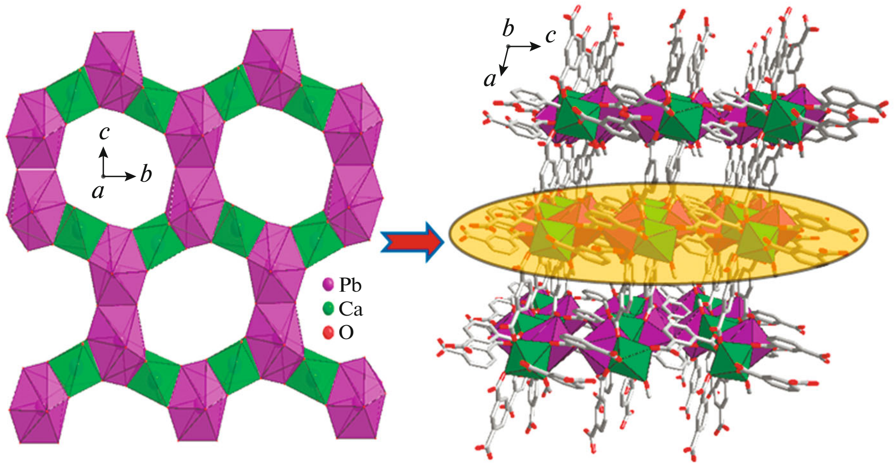

Fig. 3. The 2D inorganic Pb–O–Ca layer in **I** (a); the 3D pillar-layer framework of **I** (b).

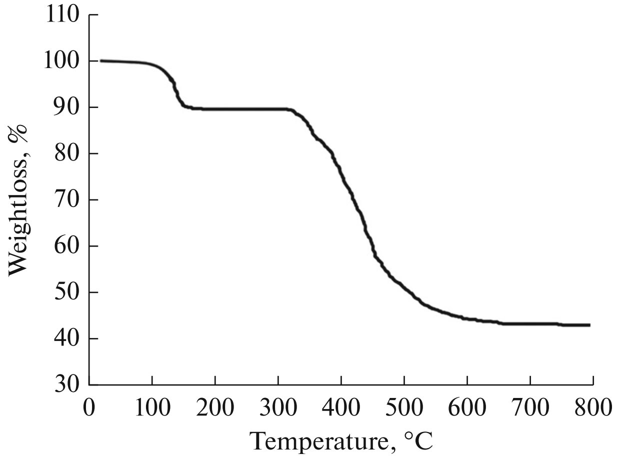

Fig. 4. The TG curve for compound **I**.

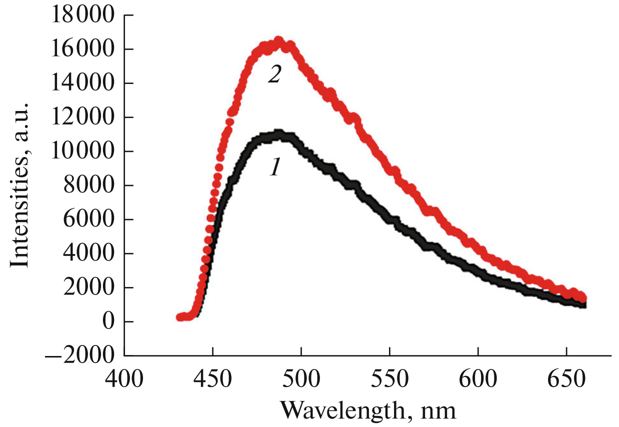

Fig. 5. The luminescent emission spectra of compound **I** (*1*) and desolvated samples (*2*) in the solid state at room temperature.

pound **I**, which indicated that the coordinated DMF molecule can cause luminescence quenching.

In summary, a new heterometallic compound has been successfully synthesized by the solvothermal reactions of $Pb(NO_3)_2$, $Ca(NO_3)_2 \cdot 4H_2O$ and H_2Mbdc. The compound exhibits a 3D pillar-layered framework with 2D inorganic Pb–O–Ca connectivity. At room temperature, this compound displays intense luminescence in the solid state. After release the coordinated DMF molecule, the desolvated samples show more intense luminescence.

ACKNOWLEDGMENTS

This work was supported by the Guangdong University of Petrochemical Technology.

REFERENCES

1. Kim, T.K., Lee, J.H., Moon, D.H., and Moon, R., *Inorg. Chem.*, 2013, vol. 53, p. 589.
2. Ding, B., Liu, S.X., Cheng, Y., et al., *Inorg. Chem.*, 2016, vol. 55, p. 4391.
3. Xu, Z.X., Tan, Y.X., Fu, H.R., et al., *Inorg. Chem.*, 2014, vol. 53, p. 12199.
4. Qi, Y.J., Zhao, D., Li, X.X., et al., *Cryst. Growth Des.*, 2017, vol. 17, p. 1159.
5. Shi, P.F., Hu, H.C., Zhang, Z.Y., et al., *Chem. Commun.*, 2015, vol. 51, p. 3985.
6. Yang, X.C. and Xu, Q., *Cryst. Growth Des.*, 2017, vol. 17, p. 1450.
7. Zhang, H.B., Lin, P., Shan, X.C., et al., *Chem. Commun.*, 2013, vol. 49, p. 2231.
8. Chen, C.X., Wei, Z., Qiu, Q.F., et al., *Cryst. Growth Des.*, 2017, vol. 17, p. 1476.
9. Foo, M.L., Horike, S., Duan, J.G., et al., *Cryst. Growth Des.*, 2013, vol. 13, p. 2965.
10. Wu, Z.F., Tan, B., Wang, J.Y., Du, S.W., et al., *Chem. Commun.*, 2015, vol. 51, p. 157.

11. Jiang, Z.Q., Jiang, G.Y., Hou, D.C., et al., *CrystEngComm*, 2013, vol. 15, p. 315.
12. Fu, H.R. and Zhang, J., *Inorg. Chem.*, 2016, vol. 55, p. 3928.
13. Xu, Y., Yuan, D.Q., Han, L., et al., *Eur. J. Inorg. Chem.*, 2005, vol. 2005, p. 2054.
14. Xu, X.X., Lu, Y., Wang, E.B., et al., *Cryst. Growth Des.*, 2006, vol. 6, p. 2029.
15. Li, X.Q., Zhang, H.B., Wu, S.T., et al., *CrystEngComm*, 2012, vol. 14, p. 936.
16. Zhang, X., Cheng, J.K., Chen, F., et al., *Inorg. Chem. Commun.*, 2011, vol. 14, p. 358.
17. Zhang, X., Cheng, J.K., Yin, P.X., and Yao, Y.G., *J. Mol. Struct.*, 2011, vol. 990, p. 1.
18. Zhang, H.X., Kang, Y., Tan, Y.X., and Zhang, J., *Inorg. Chem. Commun.*, 2011, vol. 14, p. 358.
19. Zhang, L., Qin, Y.Y., Li, Z.J., et al., *Inorg. Chem.*, 2008, vol. 47, p. 8286.
20. Thirumurugan, A., Sanguramath, R.A., and Rao, C.N.R., *Inorg. Chem.*, 2008, vol. 47, p. 823.
21. Zhang, L., Li, Z.J., Lin, Q.P., et al., *Inorg. Chem.*, 2009, vol. 48, p. 6157.
22. Zhang, X., Huang, Y.Y., Zhang, M.J., et al., *Cryst. Growth Des.*, 2012, vol. 12, p. 3231.
23. Ye, R.P., Yang, J.X., Zhang, X., and Yao, Y.G., *Z. Anorg. Allg. Chem.*, 2016, vol. 642, p. 60.
24. Wei, L.Q., Lu, J.Y., Li, Q.Q., et al., *Inorg. Chem. Commun.*, 2017, vol. 78, p. 43.
25. Lin, J.D., Wu, S.T., Li, Z.H., and Du, S.W., *CrystEngComm*, 2010, vol. 12, p. 4252.
26. Sheldrick, G.M., *SADABS*, *Program for Area Detector Adsorption Correction*, Göttingen: Univ. of Göttingen, 1997.
27. Sheldrick, G.M., *SHELXTL-97, Program for Crystal Structure Refinement*, Göttingen: Univ. of Göttingen, 1997.
28. Zhang, Y., Wang, J., Yan, X.F., et al., *Micropor. Mesopor. Mat.*, 2014, vol. 184, p. 15.
29. Lian, F.Y., Jiang, F.L., Yuan, D.Q., et al., *CrystEngComm*, 2008, vol. 10, p. 905.
30. Blasse, G. and Grabmaier, B.C., *Luminescent Materials*, Berlin: Springer, 1994.